HHS Public Access

Author manuscript

J Am Chem Soc. Author manuscript; available in PMC 2020 October 08.

Published in final edited form as:

J Am Chem Soc. 2019 August 14; 141(32): 12872–12879. doi:10.1021/jacs.9b06383.

Nickel(IV)-Catalyzed C–H Trifluoromethylation of (Hetero)arenes

Elizabeth A. Meucci[†], **Shay N. Nguyen**[†], **Nicole M. Camasso**[†], **Eugene Chong**[†], **Alireza Ariafard**[¥], **Allan J. Canty**[¥], **Melanie S. Sanford**[*,†]

[†]Department of Chemistry, University of Michigan, 930 N University Ave, Ann Arbor, MI 48109, USA

[¥]School of Physical Sciences, University of Tasmania, Hobart, Tasmania 7001, Australia

Abstract

This Article describes the development of a stable Ni^{IV} complex that mediates C(sp^2)–H trifluoromethylation reactions. This reactivity is first demonstrated stoichiometrically and then successfully translated to a Ni^{IV}-catalyzed C–H trifluoromethylation of electron-rich arene and heteroarene substrates. Both experimental and computational mechanistic studies support a radical chain pathway involving Ni^{IV}, Ni^{III}, and Ni^{II} intermediates.

Graphical Abstract

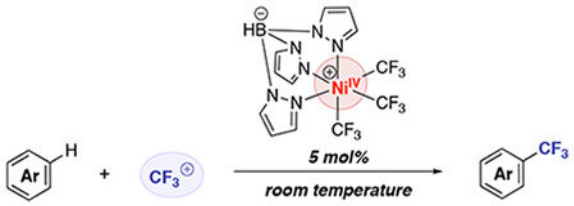

INTRODUCTION

Over the past three decades, nickel has emerged as an economical base-metal catalyst for a wide array of important chemical transformations.[1] The vast majority of these Ni-catalyzed processes are proposed to proceed via $Ni^{0/II}$, $Ni^{I/III}$ or $Ni^{I/II/III}$ catalytic cycles.[2] In many cases, these mechanisms are supported by the isolation of organonickel intermediates and studies of their catalytic competence.[3] While organonickel(I), (II), and (III) complexes are well-precedented, until 5 years ago there were very few examples of isolable Ni complexes in the +4 oxidation state.[4] As a result, Ni^{IV} intermediates have rarely been proposed in catalysis. However, recent progress by our group and others has shown that organonickel(IV) complexes can be synthesized at room temperature using mild oxidants.

[*]**Corresponding Author**: mssanfor@umich.edu.

ASSOCIATED CONTENT

Experimental details, optimization tables, and complete characterization data for all new compounds. This material is available free of charge via the Internet at http://pubs.acs.org.

The authors declare no competing financial interests.

[4b–e] Given the accessibility and unique reactivity of Ni^{IV}, we sought to investigate its relevance in catalysis.

Ni^{IV}–CF_3 complexes have been shown to exhibit superior stability when compared to other Ni^{IV}–alkyls.[5] They are also easily prepared via the net two-electron oxidation of Ni^{II} precursors with CF_3^+ oxidants (for example, see **A** in Figure 1A).[4,5] Additionally, a recent report by Nebra and coworkers demonstrated a Ni^{IV}–CF_3 complex that effects the stoichiometric C–H trifluoromethylation of 1,2-dichlorobenzene under mild conditions (Figure 1B).[6] Inspired by these results, we hypothesized that we could develop a Ni^{IV}-catalyzed method for the C–H trifluoromethylation of arenes by identifying the optimal combination of ligand, substrate, and CF_3^+ oxidant (Figure 1C).

We demonstrate herein the design and synthesis of a Ni^{IV}–CF_3 complex that participates in a net transfer of CF_3^+ to electron-rich arenes. Furthermore, in the presence of an electrophilic trifluoromethylating reagent, this Ni^{IV} complex serves as an effective catalyst for the C–H trifluoromethylation of arene and heteroarene substrates. Mechanistic studies suggest that this reaction proceeds through a $Ni^{II/III/IV}$ cycle involving CF_3 radicals as key intermediates.

RESULTS AND DISCUSSION

Design and synthesis of Ni^{IV}–CF_3 complex.

Our initial efforts focused on identifying a ligand scaffold that would enable both steps of the proposed catalytic cycle: (1) the net $2e^-$ oxidation of a Ni^{II} precursor with a "CF_3^+" oxidant to afford a Ni^{IV}–CF_3 complex and (2) the subsequent reaction of this Ni^{IV}–CF_3 with arenes to afford C(sp^2)–H trifluoromethylation products. Based on previous work from our group,[4c,5a] we hypothesized that the tris(pyrazolyl)borate (Tp) ligand would be effective in this context. Furthermore, based on Nebra's results,[6] we reasoned that the incorporation of multiple CF_3 ligands would render the resulting complex reactive towards CF_3 transfer reactions. With these considerations in mind, we initially targeted $TpNi^{IV}(CF_3)_3$ (**II**) (eq. 1).

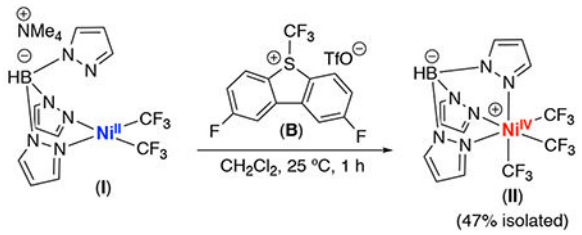

(1)

Complex **II** was synthesized via the oxidation of Ni^{II} complex **I** with 2,8-difluoro-5-(trifluoromethyl)-5*H*-dibenzo[*b,d*]thiophen-5-ium trifluoromethanesulfonate (**B**). The Ni^{IV} product was isolated in 47% yield as a yellow solid and was characterized by ^1H, ^{19}F, ^{13}C, and ^{11}B NMR spectroscopy. X-ray quality crystals were obtained by recrystallization from MeCN, and an ORTEP diagram is shown in Figure 2.

In the solid state, complex **II** is extremely stable to ambient conditions, showing no signs of decomposition after more than a year of storage on the benchtop. However, under analogous conditions as a 0.01 M solution in MeCN, **II** begins to decompose within 72 h at room temperature. Over this time, the NMR resonances associated with complex **II** gradually disappear, along with concomitant formation of CF_3H.

We next explored the reactivity of **II** in stoichiometric C(sp^2)–H trifluoromethylation. Initial studies focused on 1,2-dichlorobenzene (**1**), the substrate originally employed by Nebra (Figure 1B).[6] As shown in Table 1, entry 1, the reaction of **II** with 1 equiv of **1** afforded traces (<5%) of the C–H trifluoromethylation product **1-CF_3** after 24 h at room temperature. This yield increased to 9% when **1** was used as the reaction solvent under otherwise analogous conditions (Table 1, entry 2). We next examined the more electron rich substrate 1,3,5-trimethoxybenzene (**2**). As shown in Table 1, entry 3, complex **II** reacted with 1 equiv of **2** to afford **2-CF_3** in 47% yield as determined by ^{19}F NMR spectroscopic analysis of the crude reaction mixture. The Ni^{II} product **I-H^+** was also formed in 56% yield.[7] These yields increased to 72% and 74%, respectively, upon the use of 5 equiv of 1,3,5-trimethoxybenzene relative to **II**.

Finally, we evaluated the feasibility of regenerating Ni^{IV} complex **II** via the oxidation of **I-H^+** with **B**. As shown in eq. 2, the treatment of a solution of **I-H^+** (generated *in situ* from the reaction of **II** with 2) with 1.5 equiv of **B** afforded **II** in 63% yield after 30 s. Overall, thees studies demonstrate each individual step in the **II**-catalyzed trifluoromethylation of **2**.

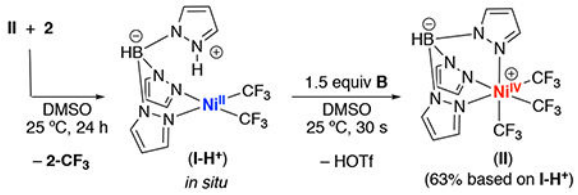

(2)

Complex II-catalyzed C–H trifluoromethylation.

We next explored the use of **II** as a catalyst for the C-H trifluoromethylation of arenes using **B** as the "CF_3^+" source.[8,9] Initial studies employed 5 mol % of **II** in combination with 1 equiv of 1,3,5-trimethoxybenzene and 1 equiv of **B** in DMSO. After 24 h at room temperature in the dark, this reaction afforded 37% yield of the C-H trifluoromethylation product **2-CF_3** (Table 2, entry 1). Importantly, no reaction was observed in the absence of complex **II** under these conditions (Table 2, entry 2). The presence/absence of ambient light did not impact the yield, ruling out a photoredox-type pathway (Table 2, entries 1 and 3). Employing complex **I** as the catalyst resulted in slightly diminished yield (25%, entry 4). The use of **A** as an oxidant also afforded a lower yield (25%, entry 5). Employing an excess of **2** (2 or 5 equiv relative to **B**) led to an increase in the yield of product **2-CF_3** (to 62% and 93%, respectively, entries 6 and 7). Optimization of the reaction time, concentration,

temperature, and solvent revealed that the highest yield of **2-CF_3** (93%) is obtained under the conditions in entry 7 (see SI for complete optimization details).

We next evaluated the scope of this **II**-catalyzed C–H trifluoromethylation. As shown in Scheme 1, this reaction proved applicable to a variety of electron-rich arene and heteroarene substrates (Scheme 1). In addition to trimethoxybenzene, electron rich pyridines as well as indole and thiophene derivatives showed good reactivity. A variety of biologically active molecules, including melatonin, Boc-L-tryptophan, resorcinol, and tadalafil, also served as effective substrates for this transformation. Notably, trifluoromethylation of tadalafil occurs at the 7-position of the indole backbone (rather than on the 1,3-dioxole-substituted ring), a site that has been functionalized in several other reported radical trifluoromethylation reactions.[10] Overall, this transformation works best with highly electron-rich (hetero)arenes, while less electron rich substrates afforded moderate to low yields (see SI for details of other substrates examined). This relatively narrow substrate scope as well as the use of 5 equiv of (hetero)arene substrate relative to oxidant represent limitations of this method compared to state-of-the-art radical C–H trifluoromethylation protocols.[11,12]

Mechanistic studies of CF_3 transfer.

We next focused on interrogating the mechanism of the CF_3 transfer step. We originally envisioned two possible pathways for this transformation (Scheme 2). The first (pathway *i*) involves a direct transfer of CF_3^+ from complex **II** to the organic substrate to form the cationic organic intermediate **13** along with the Ni^{II} product $TpNi^{II}(CF_3)_2^-$ (**I**). Intermediate **13** could then undergo deprotonation to form the trifluoromethylated product **2-CF_3** along with **I-H^+**. An alternative pathway (*ii* in Scheme 2) would proceed via release of trifluoromethyl radical from Ni^{IV} and subsequent addition of CF_3• to **2** to afford the organic intermediate **14** along with the Ni^{III} complex $TpNi^{III}(CF_3)_2$ (**III**). Compound **14** could then undergo oxidation and deprotonation to generate **2-CF_3** along with along with **I-H^+**.

To gain further insights into this transformation, we first conducted a time study, monitoring the consumption of **II** and appearance of **2-CF_3** via ^{19}F NMR spectroscopy. As shown in Figure 3, an induction period of approximately 25 min is observed, followed by rapid consumption of starting material and concomitant appearance of **2-CF_3**. This reaction profile provides initial evidence against a direct transfer of CF_3^+ from **II** (Scheme 2, i), as no induction period would be expected for this pathway.

Reaction profiles like that in Figure 3 are characteristic of radical chain processes.[13] To trap putative radical intermediates, we next carried out the reaction between **II** and **2** in the presence of TEMPO. As shown in eq. 3, the addition of 1 equiv of TEMPO inhibited productive C–H trifluoromethylation, decreasing the yield of **2-CF_3** from 72% to just 4% under otherwise analogous conditions. Furthermore, TEMPO–CF_3 (**15**, 8%) was detected by ^{19}F NMR spectroscopy.[14]

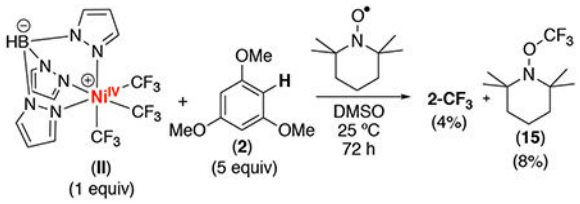

(3)

The diminished yield of **2-CF$_3$** and observation of **15** in the presence of TEMPO both implicate the intermediacy of CF_3• in this transformation. Based on the mechanism in Scheme 2, ii, this could be accompanied by the formation of the Ni^{III} intermediate **III**, a species that we have independently synthesized and characterized by EPR spectroscopy in a 3:1 mixture of PrCN:MeCN.[15] To test for the formation of **III**, we conducted the reaction between **II** and **2** and removed aliquots at several time points before, during, and after the induction period (0.5, 35, 45, and 85 min). The samples were then diluted in PrCN, and EPR spectra were acquired for each time point. As shown in Figure S45, signals consistent with a Tp-ligated Ni^{III} intermediate are observed; however, the EPR data for the major species present in these samples do not match those for **III**. This suggests that the major Ni^{III} species formed under these conditions is not complex **III**. Furthermore, as shown in eq. 3, the addition of 1 equiv of **III** to the reaction between **II** and **2** inhibited the formation of **2-CF$_3$**, with none of the product observed after 45 min.[16] Overall, these data suggest that complex **III** is not the major Ni^{III} intermediate formed under these conditions.

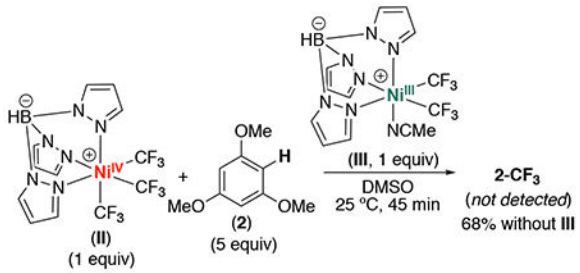

(4)

Based on these studies, we propose a radical chain mechanism for the *II*-mediated C–H trifluoromethylation of **2**. As shown in Scheme 3, i, the radical chain initiates via slow Ni^{IV}–CF_3 bond homolysis. This liberates CF_3•, which then enters the chain propagation sequence (Scheme 3, ii). Propagation is proposed to involve: (1) reaction of CF_3• with **2** to afford intermediate **14**; (2) oxidation and deprotonation of **14** by Ni^{IV} complex **II** to generate a protonated Ni^{III} intermediate **IV**; and (3) Ni^{III}–CF_3 homolysis from **IV** to release **I-H$^+$** and regenerate CF_3•. Importantly, the 17-electron Ni^{III} complex **IV** is expected to be more reactive towards Ni–CF_3 bond homolysis than the neutral, 18-electron Ni^{IV} starting material

II.[17] This should render chain propagation faster than initiation, resulting in a reaction profile like that in Figure 3.

If the mechanism in Scheme 3 is operative, then the induction period should be eliminated if the protonated (tris)trifluoromethyl Ni^{III} complex **IV** is generated independently. Based on the cyclic voltammogram of **4** (Figure S52), Cp_2Co ($E_{1/2}$ = −1.33 V vs SCE) should effect the single electron reduction of **II** ($E_{1/2}$ = –0.395 V vs SCE). In the presence of 1 equiv of TsOH•H_2O, this is expected to afford **IV**, thus chemically initiating the reaction (Scheme 4).[18]

As predicted, the addition of 0.1 equiv of Cp_2Co and 0, 0.1, or 1.0 equiv of TsOH•H_2O to the reaction between **II** and **2** under otherwise identical conditions eliminated the induction period and resulted in the steady formation of the trifluoromethylated product **2-CF_3** (Figure 4).[19] These experiments also show that the yield and rate of this reaction increases with increasing equiv of TsOH. This observation is consistent with the proposed intermediacy of the protonated Ni^{III} complex **IV**.

It was recently reported that the generation of Ni^{IV} complexes through the net 2-electron oxidation of Ni^{II} precursors can proceed via two sequential one-electron oxidations involving the formation of transient Ni^{III} intermediates.[20] If complex **II** were generated from **I** under acidic conditions via this type of pathway, Ni^{III} species **IV** would be a likely intermediate (Scheme 5). We explored this possibility by examining the time course of **2-CF_3** formation, using a combination of 1 equiv of Ni^{II} complex **I**, 1 equiv of **B**, and 1 equiv TsOH•H_2O to mediate the C–H trifluoromethylation of **2**. As shown in Figure 5, using **I**/**B**/TsOH, the reaction showed no induction period, and **2-CF_3** was formed in 70% yield within 1 h at room temperature.

The results in Figure 5 can be rationalized based on the formation of the protonated Ni^{III} intermediate **IV** during oxidation of **I**. We propose that **IV** then rapidly expels CF_3• to initiate the reaction and enter the propagative cycle. However, notably, our proposed mechanism also implicates the intermediacy of Ni^{IV} complex **II**, which serves as an oxidant during propagation. Consistent with this proposal, ^{19}F NMR spectroscopic monitoring of the trifluoromethylation of **2** with **I/B** showed that the Ni largely rests as Ni^{IV} complex **II** during this transformation (Figure S48). This Ni^{IV} complex persists throughout the product-forming stage, decaying at a rate that is similar to the rate of **2-CF_3** formation. These results are mirrored in the catalytic variant of this reaction (see SI for details).

DFT studies of CF_3 transfer from complex II.

We next examined the feasibility of the proposed pathway using DFT calculations.[21] Gaussian 09 was used at the B3LYP[22] level of density functional theory (DFT) for geometry optimization (see SI for complete details). Figure 6 illustrates the energy profile for propagation obtained following the initiation step that forms CF_3 radical.

The addition of CF_3• to **2** to afford **14** is downhill by −6.6 kcal/mol (with $\Delta G^{\dagger}$ = 7.7 kcal/mol). The organic radical **14** exhibits a distorted tetrahedral geometry at the "C(H)(CF_3)C_2" center. As anticipated for p-delocalization, the C–C_{ortho} bonds are ~0.1 Å longer than those

between the other carbon atoms, and the SOMO exhibits p-character located on these carbon and adjacent oxygen atoms. Compound **14** can undergo a highly favorable [DG (ΔH) = −30.5 (−36.8) kcal/mol] electron transfer with Ni^{IV} complex **II** to afford the arenium/Ni^{III} pair **V** in a barrierless process. Structure **V** exhibits a weak interaction between the organic fragment and a nitrogen atom coordinated to Ni (N·····H = 2.796 Å). Spin density for **V** is located primarily at Ni (0.82 e/$Å^3$), and the SOMO is an antibonding orbital located in the Ni coordination sphere (Figure 7). This is consistent with electron transfer from **14** to nickel to give Ni^{III} and an arenium fragment.

The sequence **V** → **IV** was obtained by initially locating transition state **TS-VI/IV**, followed by potential energy scans and optimizations from this structure. Notably, barriers within this sequence are very low: $\Delta G^{\dagger}$ = 3.2 and 7.3 kcal/mol). Dissociation of the axial pyrazole occurs via transition state **TS-V/VI** to give **VI**, followed by proton transfer via transition state **TS-VI/IV** to afford a weak adduct that dissociates to form organic product **2-CF_3** and square-pyramidal Ni^{III} (**IV**). Consistent with the formulation of **IV** as a Ni^{III} complex, spin-density is located primarily at Ni (Ni 0.68 e/$Å^3$, C_{axial} 0.28 e/$Å^3$) and a LUMO can be readily assigned as Ni–C s* (Figure 7). Computation for loss of CF_3• from **IV** to give the diamagnetic Ni^{II} product **I-H^+** led to detection of transition state **TS-IV/I-H**+ for CF_3• dissociation.

Overall, these calculations show that the proposed steps of the propagative sequence have low barriers (<14.4 kcal/mol for **IV** → **I-H^+**) and are thus expected to be fast at 25 °C. We next turned our focus on the initiation step. A transition state for the formation of $TpNi^{III}(CF_3)_2$ and CF_3• from **II** could not be detected computationally. Thus, in accord with the protocol presented by Hartwig and Hall,[23] the Gibbs initiation barrier is estimated as ~ΔH, i.e. $\Delta G^{\ddagger}$ ~ 17.9 kcal/mol. This barrier is significantly higher than that for **IV** ® **I-H^+** (14.4 kcal/mol), consistent with the proposed mechanism. In addition to experimental evidence for a higher barrier for initiation versus propagation, the initiation step computes as endergonic (ΔG = 3.4 kcal/mol) and only slightly favorable after solvation to form **III** ligated by DMSO ($\Delta G^{\ddagger}$ = −0.5 kcal/mol).

These studies support the challenging release of CF_3• from complex **II**. This is consistent with the induction period observed in both stoichiometric and catalytic reactions that start with Ni^{IV} complex **II**. Subsequent entrance into the proposed propagative regime through the addition of CF_3• to trimethoxybenzene represents a transition into a much lower energy phase of the reaction profile. In summary, these computations provide additional support for the proposed radical chain mechanism involving an energy-intensive initiation event that then provides access to a more favorable propagative regime. The Ni^{IV}-catalyzed C–H trifluoromethylation reaction is expected to have analogous initiation and propagation as the stoichiometric variant. The reaction then turns over via the oxidation and deprotonation of **I-H^+** with the CF_3^+ reagent **B**.

SUMMARY AND CONCLUSIONS

In conclusion, this study represents the first example where Ni^{IV} intermediates are implicated spectroscopically in catalysis. Detailed experimental and computational studies

of the trifluoromethylation of trimethoxybenzene mediated by complex **II** support a radical chain pathway in which this Ni^{IV} intermediate plays a role in both the initiation and propagation regimes. Future work will investigate the use of Ni^{IV} as a mild source of other carbon-centered radicals. Ultimately, we anticipate that the insights acquired in this study will inform the development of novel reactions involving Ni^{IV} intermediates.

Supplementary Material

Refer to Web version on PubMed Central for supplementary material.

ACKNOWLEDGMENTS

This work was supported by the National Science Foundation (NSF) Grant CHE-1111563, the Australian Research Council, and the Australian National Computing Infrastructure. We also thank Rackham Graduate School and the NSF for graduate fellowships to E.A.M, the NSF for a REU summer fellowship for S.N.N., and the NSERC for a postdoctoral fellowship for E.C. We gratefully acknowledge Dr. Jeff Kampf for X-ray crystallographic analysis of complex **II**, as well as funding from NSF Grant CHE-0840456 for X-ray instrumentation.

REFERENCES

1. (a)Tasker SZ; Standley EA; Jamison TF Recent advances in homogeneous nickel catalysis. Nature 2014, 509, 299–309. [PubMed: 24828188] (b)Ananikov VP Nickel: The “spirited horse” of transition metal catalysis. ACS Catal. 2015, 5, 1964–1971.(c)Keim W Nickel: an element with wide application in industrial homogeneous catalysis. Angew. Chem., Int. Ed 1990, 29, 235–244. (d)Rosen BM; Quasdorf KW; Wilson DA; Zhang N; Resmerita A-M; Garg NK; Percec V Nickel-catalyzed cross-coupling involving carbon–oxygen bonds. Chem. Rev 2011, 111, 1346–1416. [PubMed: 21133429]
2. (a)Montgomery J, in Organometallics in Synthesis: Fourth Manual, B. H. Lipschutz, Ed. (Wiley, Hoboken, NJ, 2013), pp. 319–428.(b)Hu X Nickel-catalyzed cross coupling of non-activated alkyl halides: a mechanistic perspective. Chem. Sci 2011, 2, 1867–1886.
3. For some examples, see:(a)Tsou TT; Kochi JK Mechanism of oxidative addition. Reaction of nickel(0) complexes with aromatic halides. J. Am. Chem. Soc 1979, 101, 6319–6332.(b)Laskowski CA; Bungum DJ; Baldwin SM; Del Ciello SA; Iluc VM; Hillhouse GL Synthesis and reactivity of two-coordinate Ni(I) alkyl and aryl complexes. J. Am. Chem. Soc 2013, 135, 18272–18275. [PubMed: 24237257] (c)Grove DM; van Koten G; Zoet R Unique stable organometallic nickel(III) complexes: syntheses and molecular structure of $Ni[C_6H_3(CH_2NMe_2)_2\text{-}o,o']_2I_2$. J. Am. Chem. Soc 1983, 105, 1380–1381.
4. For select examples of Ni^{IV} complexes that have been isolated and studied, see:(a)Klein H-F; Bickelhaupt A; Jung T; Cordier G Syntheses and properties of the first octahedral diorganonickel(IV) compounds. Organometallics, 1994, 13, 2557–2559.(b)Dimitrov V; Linden A A pseudotetrahedral, high-oxidation-state organonickel compound: synthesis and structure of bromotris(1-norbornyl)nickel(IV). Angew. Chem., Int. Ed 2003, 42, 2631–2633.(c)Camasso NM; Sanford MS Design, synthesis, and carbon-heteroatom coupling reactions of organometallic nickel(IV) complexes. Science 2015, 347, 1218–1220. [PubMed: 25766226] (d)Martinez GE; Ocampo C; Park YJ; Fout AR Accessing pincer bis(carbene) Ni(IV) complexes from Ni(II) via halogen and halogen surrogates. J. Am. Chem. Soc 2016, 138, 4290–4293. [PubMed: 27014933] (e)Schultz JW; Fuchigami K; Zheng B; Rath NP; Mirica LM Isolated organometallic nickel(III) and nickel(IV) complexes relevant to carbon-carbon bond formation reactions J. Am. Chem. Soc 2016, 138, 12928–12934. [PubMed: 27599205]
5. (a)Bour J; Camasso NM; Sanford MS Oxidation of Ni(II) to Ni(IV) with aryl electrophiles enables Ni-mediated aryl–CF_3 coupling. J. Am. Chem. Soc 2015, 137, 8034–8037. [PubMed: 26079544] (b)Chong E; Kampf JW; Ariafard A; Canty AJ; Sanford MS Oxidatively induced C-H activation at high valent nickel. J. Am. Chem. Soc 2017, 139, 6058–6061. [PubMed: 28425702] (c)Zhang C-P; Wang H; Klein A; Biewer C; Stirnat K; Yamaguchi Y; Xu L; Gomez-Benitez V; Vicic DA A five-

coordinate nickel(II) fluoroalkyl complex as a precursor to a spectroscopically detectable Ni(III) species. J. Am. Chem. Soc 2013, 135, 8141–8144. [PubMed: 23692548]

6. D'Accriscio F; Borja P; Saffon-Merceron N; Fustier-Boutignon M; Mézailles N; Nebra N C–H bond trifluoromethylation of arenes enabled by a robust, high-valent Ni^{IV} complex. Angew. Chem., Int. Ed 2017, 56, 12898–12902.
7. The identity of Ni^{II} product **I-H**$^{+}$ was confirmed by comparing the ^{19}F NMR shift observed for the Ni^{II} product of this reaction to the signal generated upon treatment of Ni^{II} complex **I** with TsOH in DMSO. See SI for details.
8. (a)Umemoto T; Zhang B; Zhu T; Zhou X; Zhang P; Hu S; Li Y Powerful, thermally stable, one-pot-preparable, and recyclable electrophilic trifluoromethylating agents: 2,8-difluoro- and 2,3,7,8-tetrafluoro-*S*-(trifluoromethyl)bibenzothiophenium salts. J. Org. Chem 2017, 82, 7708–7719. [PubMed: 28541682] (b)Egami H; Ito Y; Ide T; Masuda S; Hamashima Y Simple photo-induced trifluoromethylation of aromatic rings. Synthesis 2018, 50, 2948–2953.
9. Gao X; Geng Y; Han S; Liang A; Li J; Zou D; Wu Y; Wu Y Nickel-catalyzed direct C–H trifluoromethylation of free anilines with Togni's reagent. Org. Lett 2018, 20, 3732–3735. [PubMed: 29920105]
10. (a)Rey-Rodriguez R; Retailleau P; Bonnet P; Gillaizeau I Iron-catalyzed trifluoromethylation of enamide. Chem. Eur. J 2015, 21, 3572–3575. [PubMed: 25611040] (b)Jacquet J; Blanchard S; Derat E; Desage-El Murr M; Fensterbank L Redox-ligand sustains controlled generation of CF_3 radicals by well-defined copper complex. Chem. Sci 2016, 7, 2030–2036. [PubMed: 29899928] (c)Chang B; Shao H; Yan P; Qiu W; Weng Z; Yuan R Quinone-mediated trifluoromethylation of arenes and heteroarenes with visible light. ACS Sustainable Chem. Eng 2017, 5, 334–341.
11. Nagib DA; MacMillan DWC Trifluoromethylation of arenes and heteroarenes by means of photoredox catalysis. Nature 2011, 480, 224–228. [PubMed: 22158245]
12. Ji Y; Brueckl T; Baxter RD; Fujiwara Y; Seiple IB; Su S; Blackmond DG; Baran PS Innate C-H trifluoromethylation of heterocycles. Proc. Nat. Acad. Sci 2011, 108, 14411–14415. [PubMed: 21844378]
13. Helfferich FG Chain Reactions In Comprehensive Chemical Kinetics. Elsevier Science B.V.: Amsterdarm, The Netherlands 2001; Vol. 38, pp 263–297.
14. (a)Seo S; Taylor JB; Greaney MF Silver-catalysed trifluoromethylation of arenes at room temperature. Chem. Commun 2013, 49, 6385–6387.(b)Chen S; Feng D-F; Li D-Y; Liu P-N Radical cyanotrifluoromethylation of isocyanides: step-econmoical access to CF_3-containing nitriles, amines, and imines. Org. Lett 2018, 20, 5418–5422. [PubMed: 30148642] (c)Liang A; Han S; Liu Z; Wang L; Zou D; Wu Y; Wu Y Regioselective synthesis of N-heteroaromatic trifluoromethoxy compounds by direct O–CF_3 bond formation. Chem. Eur. J 2016, 22, 5102–5106. [PubMed: 26791812]
15. Bour JB; Camasso NM; Meucci EA; Kampf JW; Canty AJ; Sanford MS Carbon-carbon bond-forming reductive elimination from isolated nickel(III) complexes. J. Am. Chem. Soc 2016, 138, 16105–16111. [PubMed: 27960311]
16. We investigated the possible role of the MeCN ligand on **III** by adding and removing (via vacuum) CH_2Cl_2 from **III** several times. The resulting complex was also observed to severely inhibit the trifluoromethylation of **2** by **II**. The trifluoromethylation of **2** catalyzed by **II** performs similarly in MeCN and DMSO. These data suggest that the MeCN on **III** does not inhibit the reaction.
17. (a)Tilset M One-electron oxidation of cyclopentadienylchromium carbonyl hydrides: thermodynamics of oxidative activation of metal-hydrogen bonds toward homolytic and heterolytic cleavage. J. Am. Chem. Soc 1992, 114, 2740–2741.(b)Skagestad V; Tilset M Thermodynamics of heterolytic and homolytic metal-hydrogen bond cleavage reactions of 18-electron and 17-electron group 6 hydridotris(pyrazolyl)borate metal hydrides. J. Am. Chem. Soc 1993, 115, 5077–5083. (c)Tilset M; Hamon J-R; Hamon P Relative M–X bond dissociation energies in 16-, 17- and 18-electron organotransition-metal complexes (X = halide, H). Chem. Commun 1998, 765–766.
18. Connelly NG; Geiger WE Chemical redox agents for organometallic chemistry. Chem. Rev 1996, 96, 877–910. [PubMed: 11848774]
19. Attempts to utilize Cp_2Co and T sOH to initiate the catalytic reaction did not result in higher yields, see SI for details.

20. Bour JR; Ferguson DM; McClain EJ; Kampf JW; Sanford MS Connecting organometallic Ni(III) and Ni(IV): Reactions of carbon-centered radicals with high-valent organonickel complexes. J. Am. Chem. Soc 2019, 141, 8914–8920. [PubMed: 31136162]

21. Frisch MJ; Trucks GW; Schlegel HB; Scuseria GE; Robb MA; Cheeseman JR; Scalmani G; Barone V; Mennucci B; Petersson GA; Nakatsuji H; Caricato M; Li X; Hratchian HP; Izmaylov AF; Bloino J; Zheng G; Sonnenberg JL; Hada M; Ehara M; Toyota K; Fukuda R; Hasegawa J; Ishida M; Nakajima T; Honda Y; Kitao O; Nakai H; Vreven T; Montgomery JA Jr.; Peralta JE; Ogliaro F; Bearpark M; Heyd JJ; Brothers E; Kudin KN; Staroverov VN; Kobayashi R; Normand J; Raghavachari K; Rendell A; Burant JC; Iyengar SS; Tomasi J; Cossi M; Rega N; Millam JM; Klene M; Knox JE; Cross JB; Bakken V; Adamo C; Jaramillo J; Gomperts R; Stratmann RE; Yazyev O; Austin AJ; Cammi R; Pomelli C; Ochterski JW; Martin RL; Morokuma K; Zakrzewski VG; Voth GA; Salvador P; Dannenberg JJ; Dapprich S; Daniels AD; Farkas O; Foresman JB; Ortiz JV; Cioslowski J; and Fox DJ Gaussian 09, revision A.02; Gaussian, Inc.; Wallingford CT, 2009.

22. Lee CT; Yang WT; Parr RG Development of the Colle-Salvetti correlation-energy formula into a functional of the electron density. Phys. Rev. B 1988, 37, 785–789.(b)Miehlich B; Savin A; Stoll H; Preuss H Results obtained with the correlation energy density functionals of becke and Lee, Yang and Parr. Chem. Phys. Lett 1989, 157, 200–206.(c)Becke AD Density-functional thermochemistry. III. The role of exact exchange. J. Chem. Phys 1993, 98, 5648–5652.

23. (a)Hartwig JF; Cook KS; Hapke M; Incarvito CD; Fan Y; Webster CE; Hall MB Rhodium boryl complexes in the catalytic, terminal functionalization of alkanes. J. Am. Chem. Soc 2005, 127, 2538–2552. [PubMed: 15725009] (b)Wei CS; Jimenez-Hoyos CA; Videa MF; Hartwig JF; Hall MB Origins of the selectivity for borylation of primary over secondary C–H bonds catalyzed by Cp*-Rhodium complexes. J. Am. Chem. Soc 2010, 132, 3078–3091. [PubMed: 20121104]

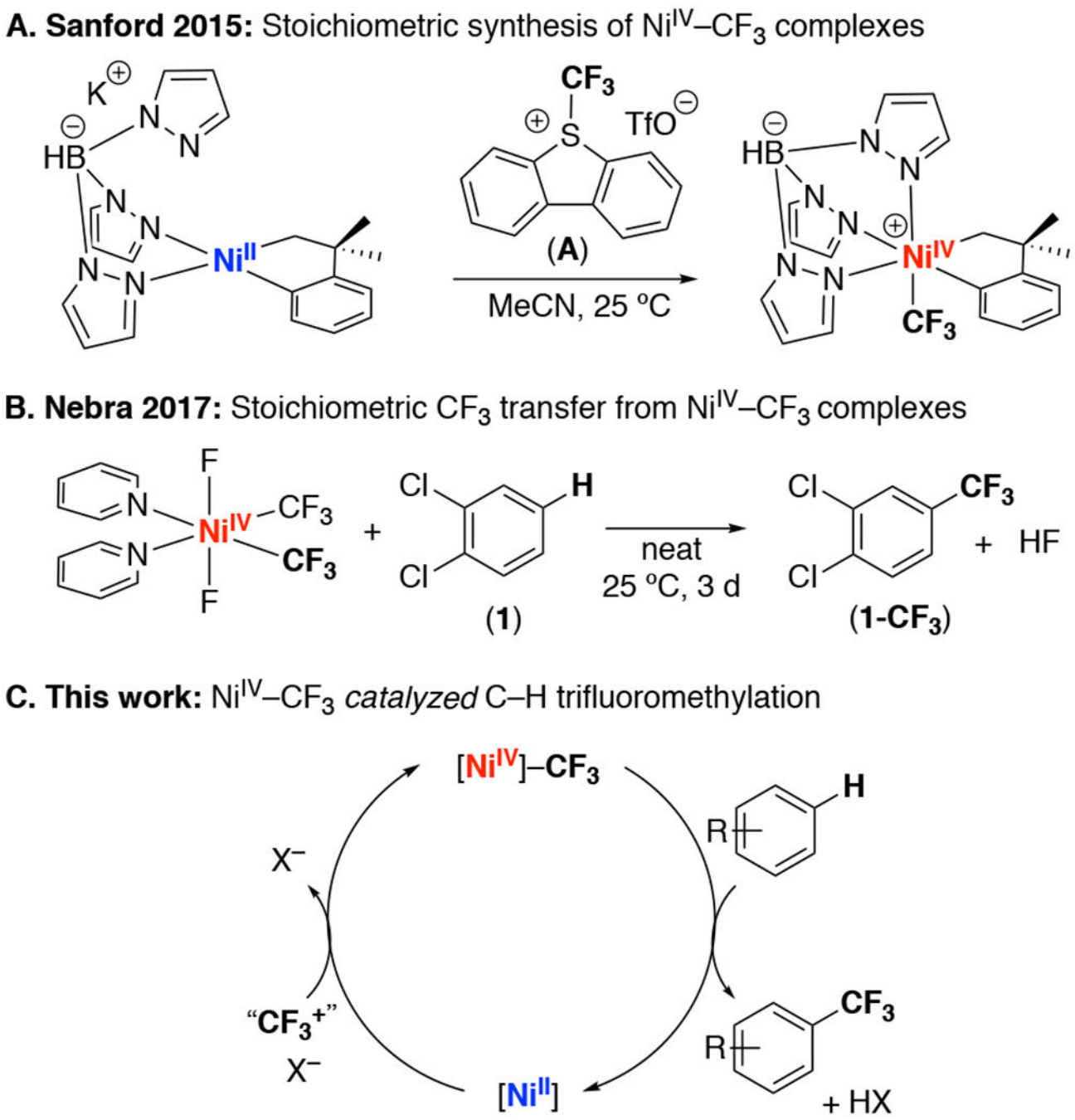

Figure 1.

(A) Synthesis of Ni^{IV}–CF_3 complexes. (**B**) Stoichiometric C(sp^2)-H trifluoromethylation mediated by Ni^{IV}. (**C**) Overall cycle for Ni^{IV}-catalyzed trifluoromethylation.

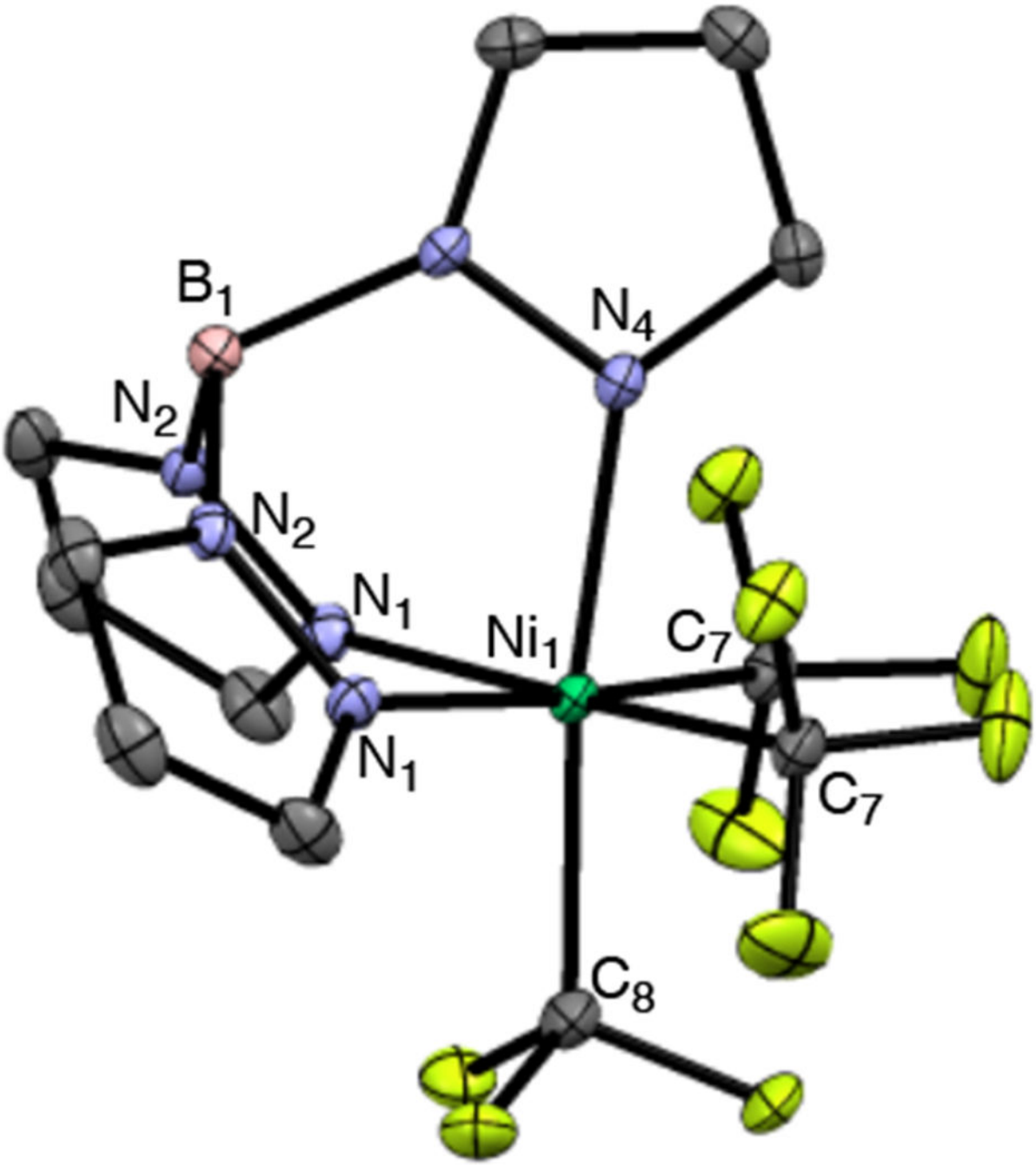

Figure 2.

ORTEP diagram for complex **II**. Hydrogen atoms have been omitted for clarity, thermal ellipsoids drawn at 50% probability. Bond lengths (Å): Ni_1–N_1 = 2.013, Ni_1–N_4 = 1.974, Ni_1–C_7 = 2.011, Ni_1–C_8 = 1.983 and bond angles (deg): C_7–Ni_1–C_7 = 99.81, C_7–Ni_1–C_8 = 88.05.

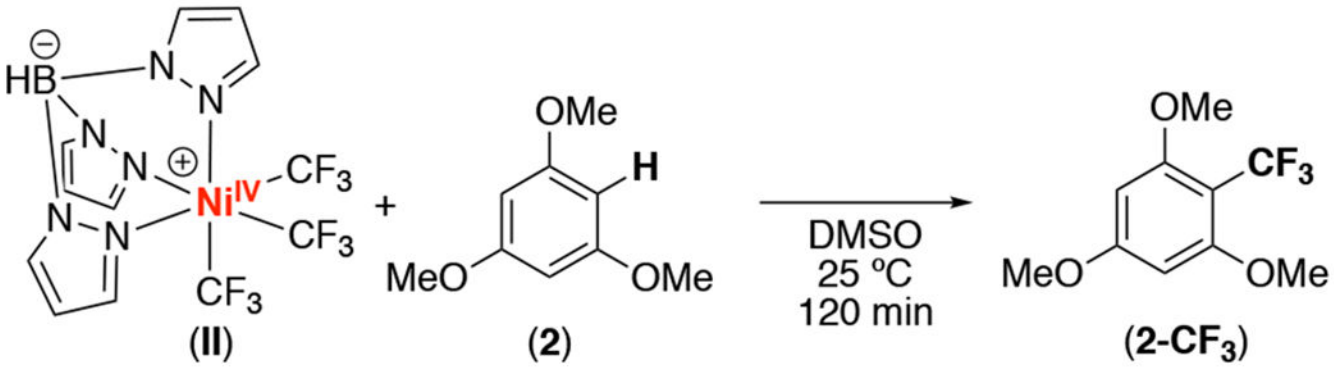

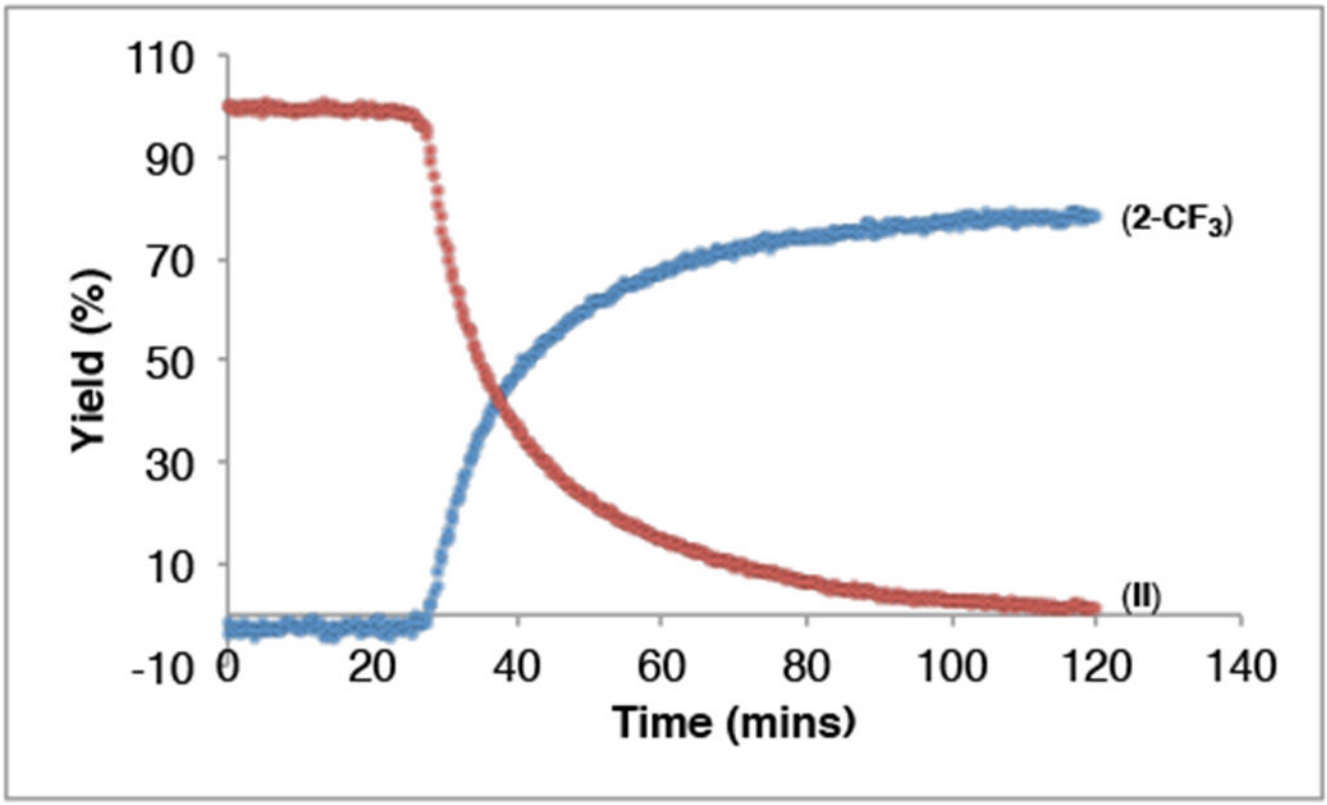

Figure 3.

Reaction profile for the trifluoromethylation of trimethoxybenzene with complex **II**. Reaction conducted with 1.0 equiv **II** and 5.0 equiv **2**.

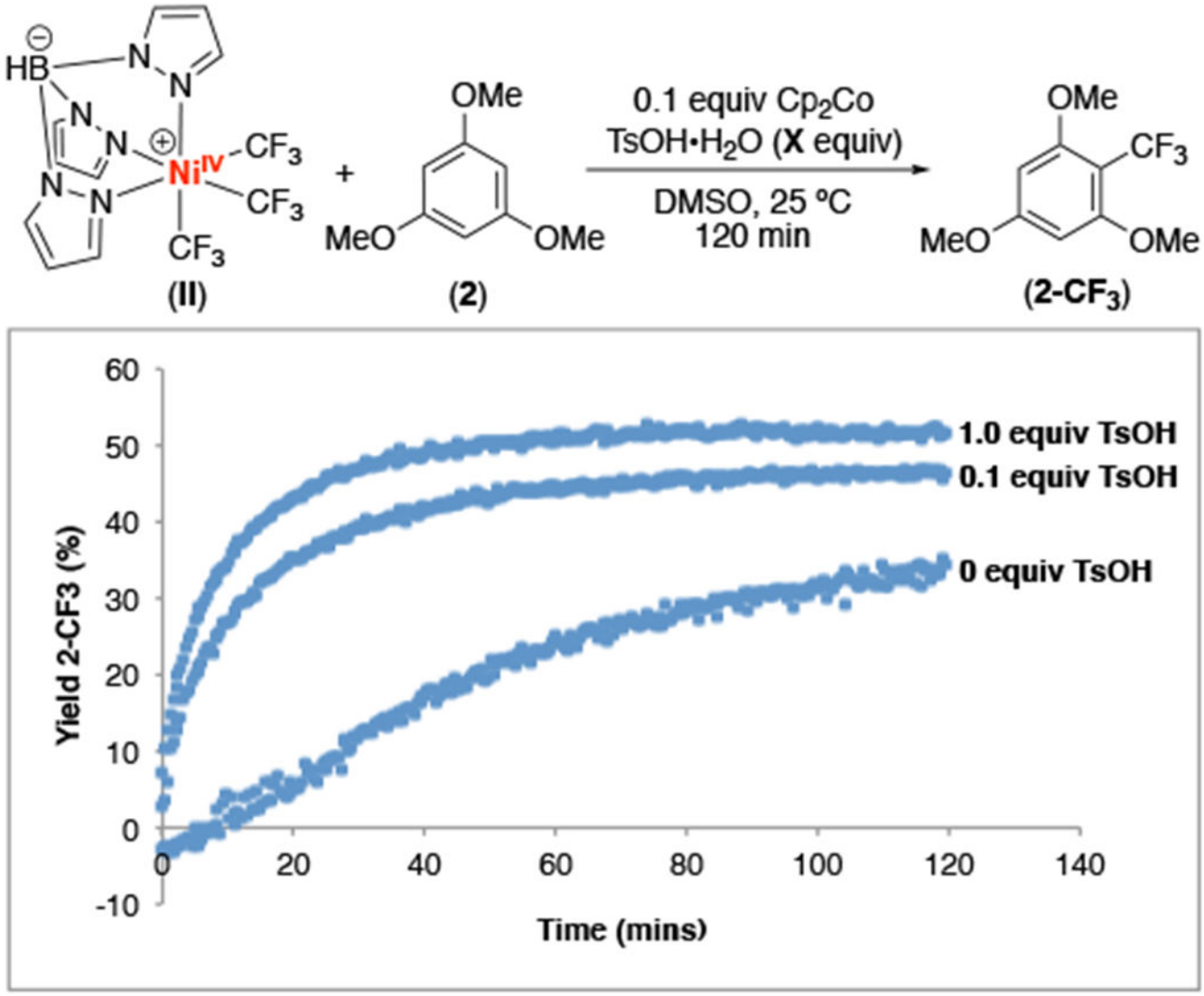

Figure 4.

Reaction profile for the trifluoromethylation of trimethoxybenzene with complex **II** in the presence of Cp_2Co and TsOH. Reaction conducted with 1.0 equiv **II**, 5.0 equiv **2**, 0.1 equiv Cp_2Co, and varied equiv of TsOH•H_2O. Cp_2Co was added to **II** and **2** immediately before the addition of TsOH•H_2O.

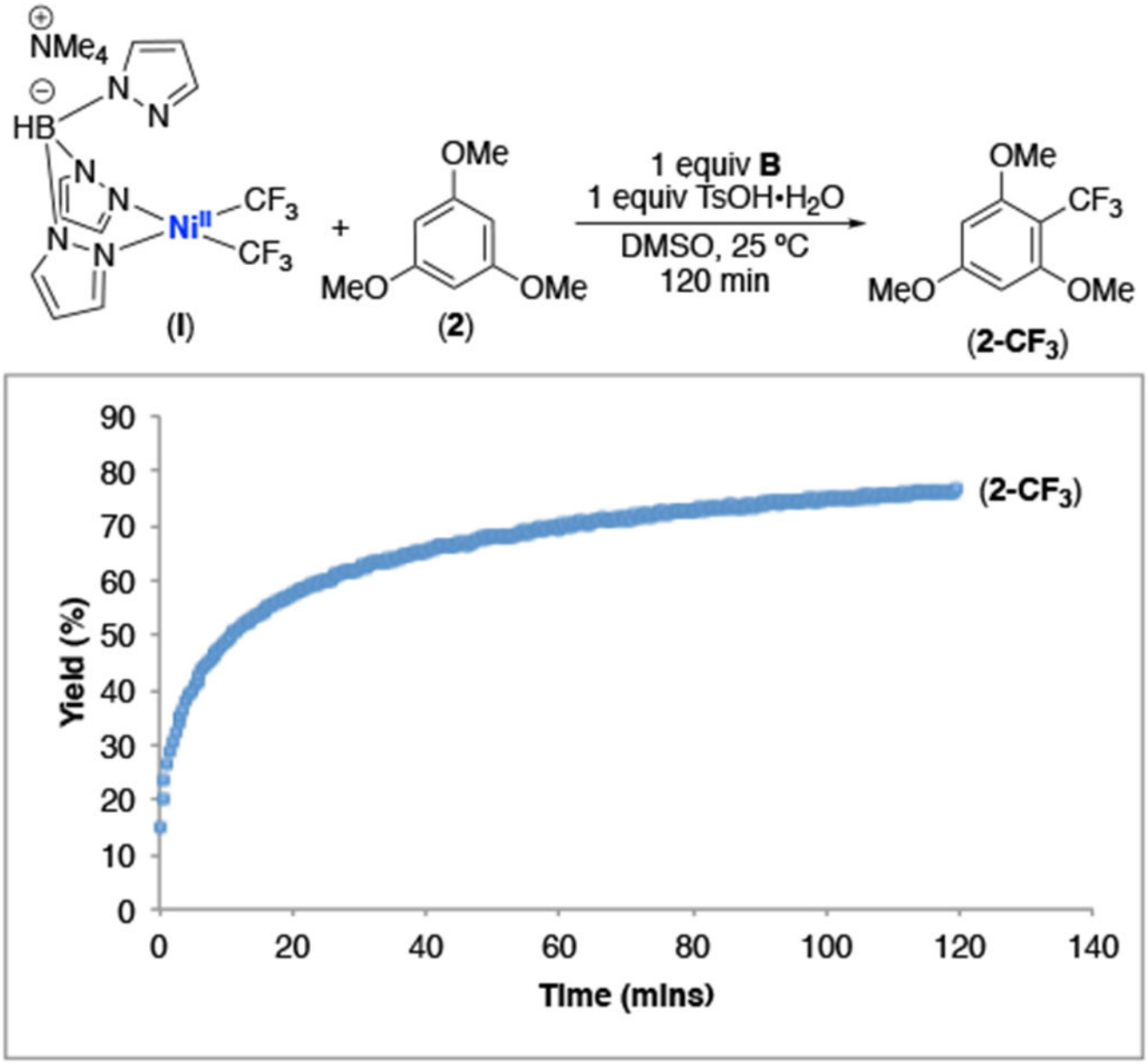

Figure 5.

Reaction profile for the trifluoromethylation of trimethoxybenzene meditated by complex **I** in the presence of **B** and TsOH. Reaction conducted with 1.0 equiv **I**, 5.0 equiv **2**, 1.0 equiv **B**, and 1.0 equiv TsOH•H_2O. **B** was added to **I** and **2** immediately before the addition of TsOH•H_2O.

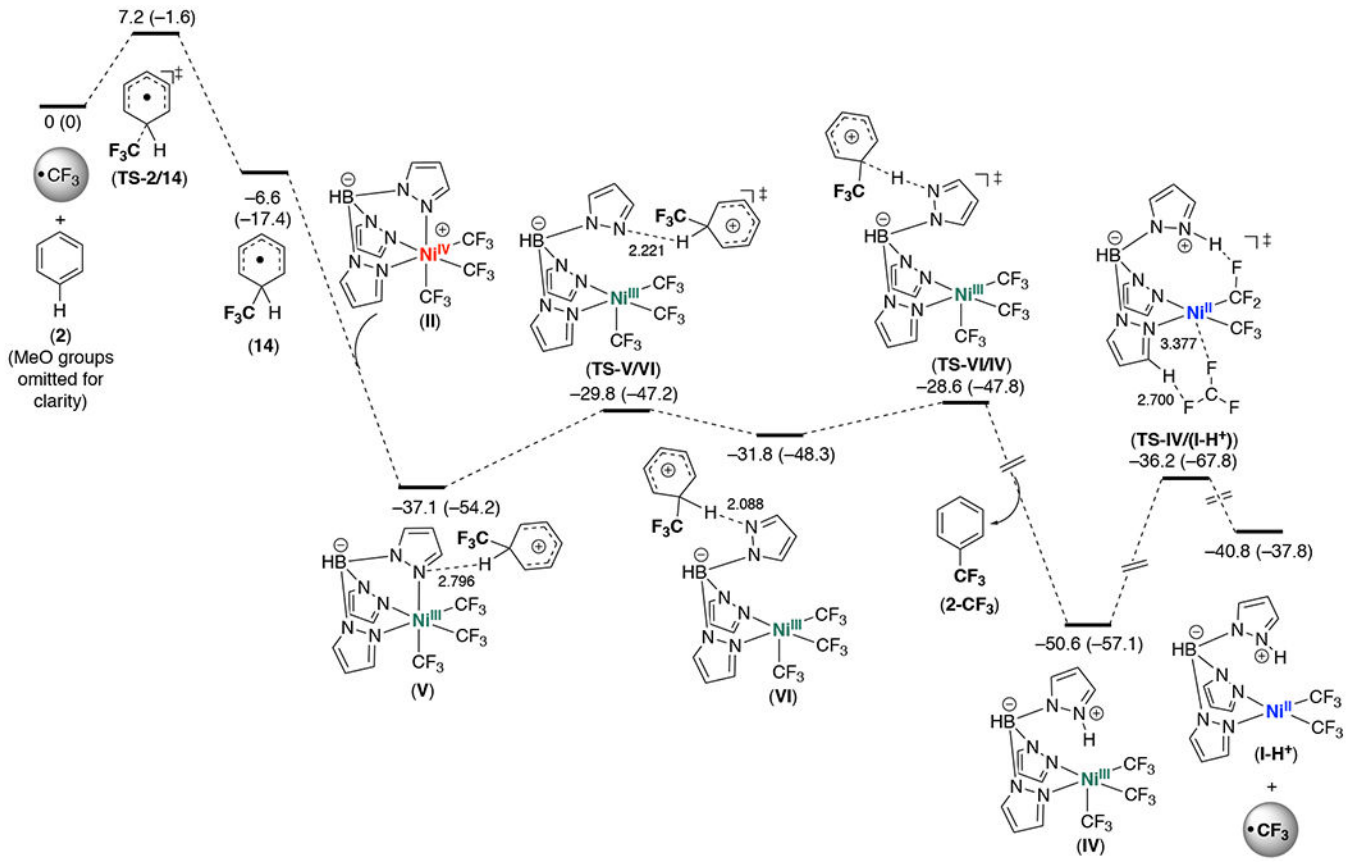

Figure 6.

Energy profile for the propagation steps in the reaction of $TpNi^{IV}(CF_3)_3$ (**II**) with 1,3,5-trimethoxybenzene (**2**). Methoxy groups are omitted for clarity. Details for additional species: adduct after **TS-VI/IV** (−48.8 (−67.3)), conformer after **IV** formed by pyrazole rotation (−46.9 (−55.0), and adduct after **VII** (−36.1 (−40.7)) are provided in Supporting Information. Distances for selected interatomic interactions are given in Å. Energies ΔG (ΔH) in kcal/mol are relative to (CF_3• + **2**).

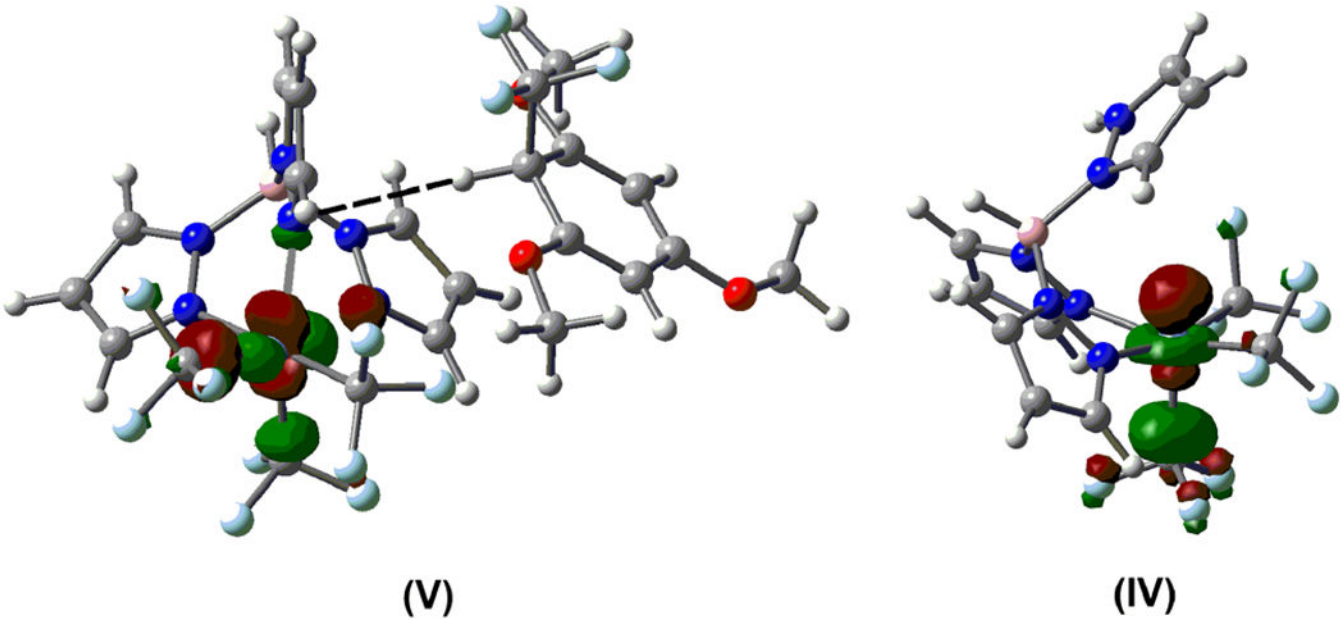

Figure 7.
Nickel-centered SOMOs for **V** and **IV**, illustrating nickel-centered antibonding character in both structures.

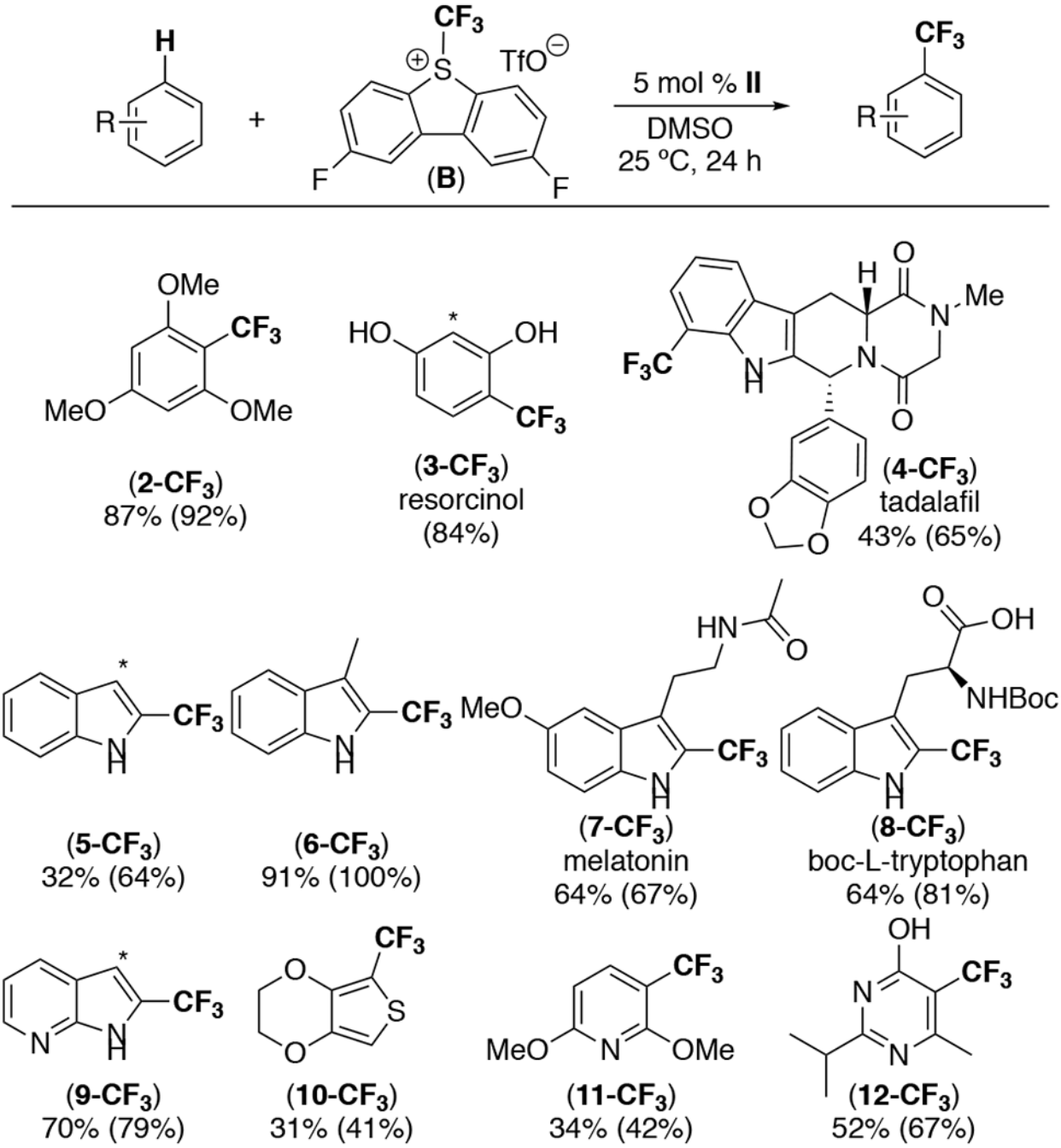

Scheme 1.

Scope of Ni^{IV}-catalyzed trifluoromethylation[a]

[a] General conditions: 1.0 equiv **B**, 5.0 equiv arene, 5 mol % of **II** in DMSO for 24 h at 25 °C. ^{19}F NMR yields are in parentheses and were determined using trifluorotoluene as an internal standard. In cases where multiple isomers were formed, NMR yield is given as a combined yield. *Signifies the site of a minor isomer.

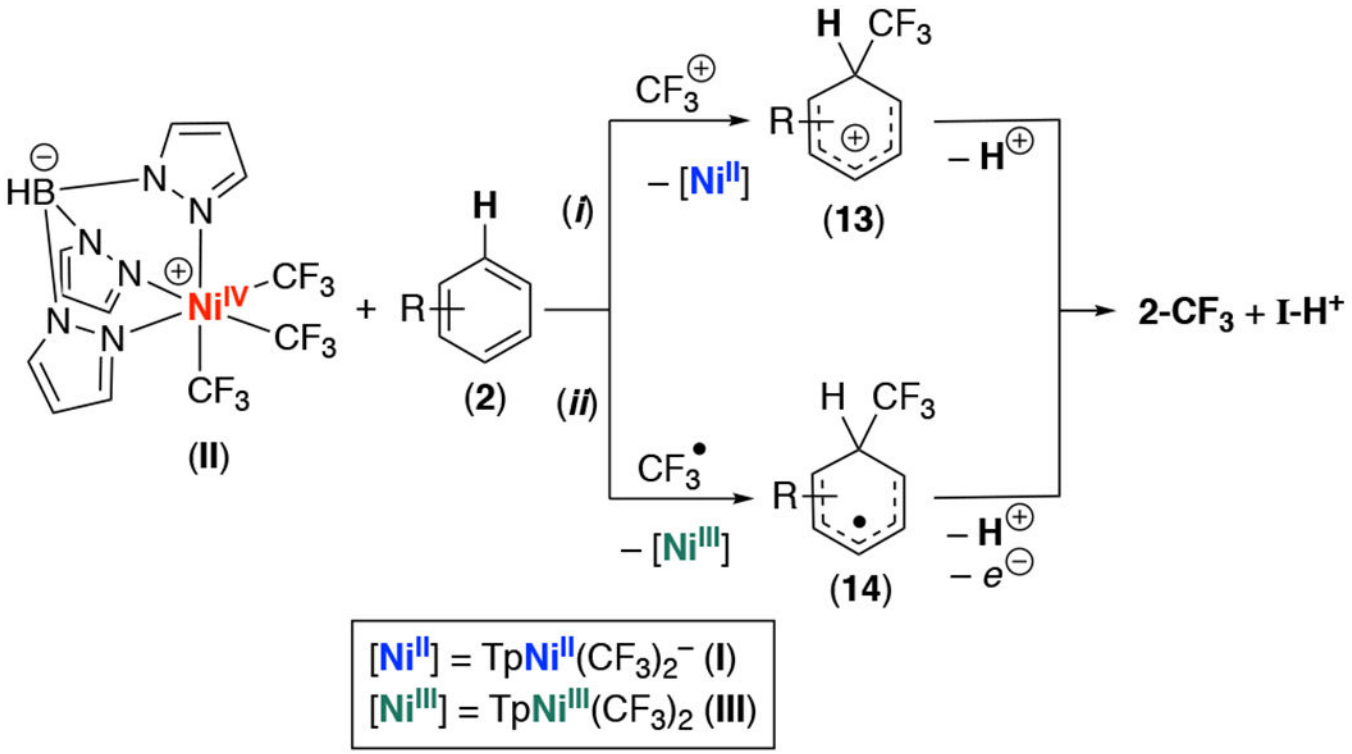

Scheme 2.

Two possible mechanisms for CF_3 transfer from **II**

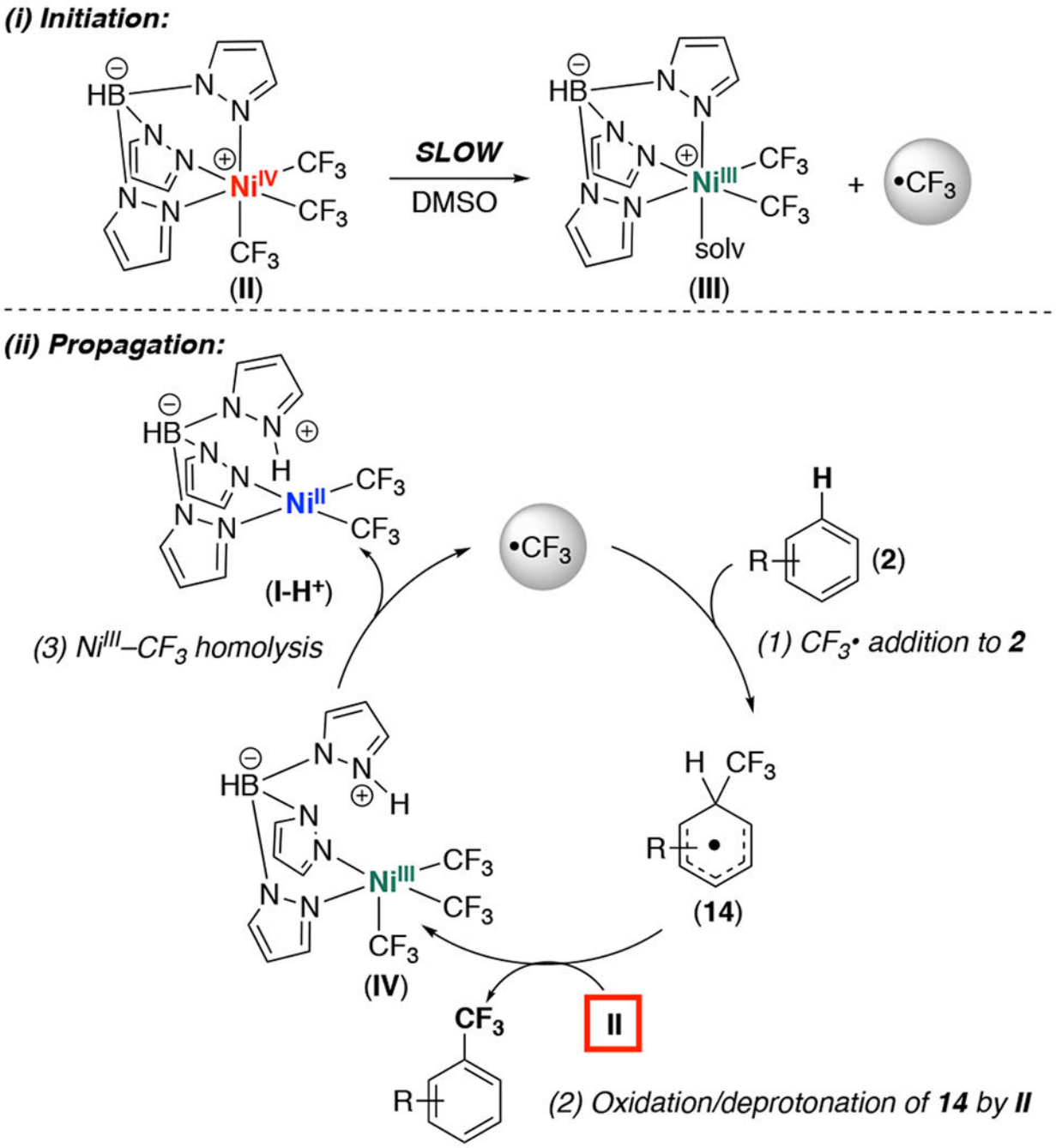

Scheme 3.

Proposed radical chain pathway for **II**-mediated C–H trifluoromethylation

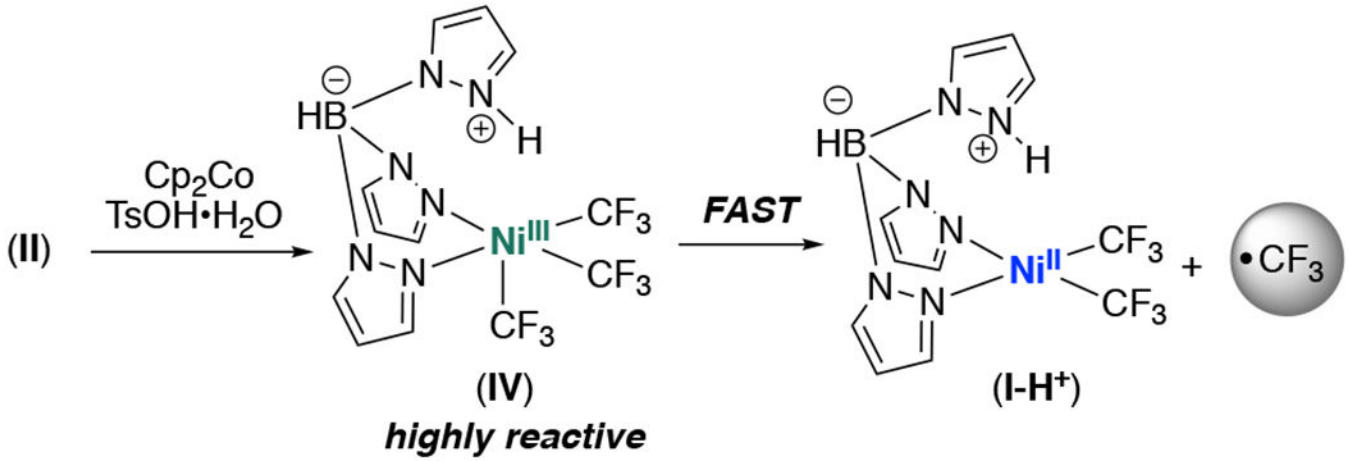

Scheme 4.
Reduction of **II** as a route to CF_3•

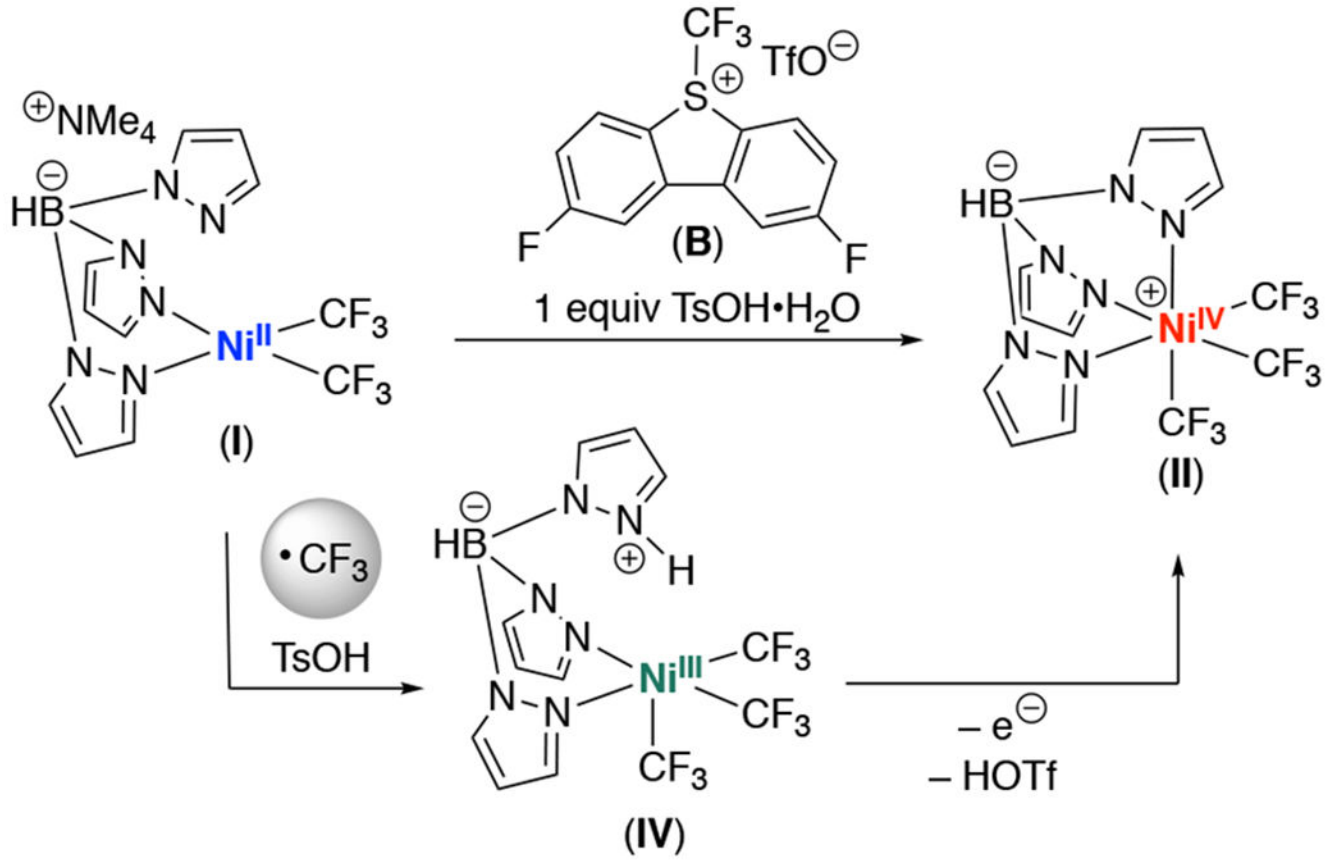

Scheme 5.
Proposed sequential single electron oxidation step to convert **I** to **II** in the presence of TsOH

Table 1.

Reactions of **II** with Ar–H substrates.

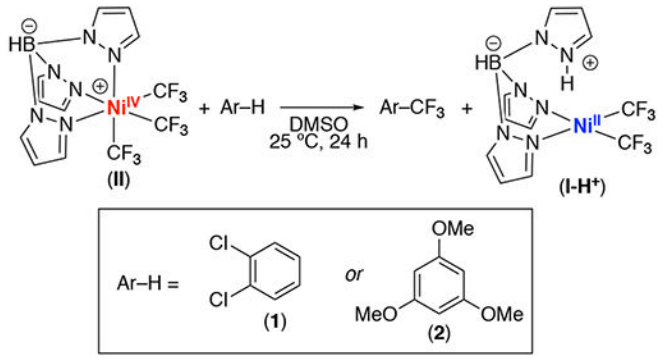

entry	Ar-H	equiv Ar–H	yield (%)[a]
1	**1**	1 equiv	trace
2	**1**	neat	9[b]
3	**2**	1 equiv	47
4	2	5 equiv	72

[a]Yields determined by ^{19}F NMR spectroscopy using trifluorotoluene as an internal standard and are based on **II**. All reactions conducted using 1.0 equiv **II**.

[b]1 : 1.2 ratio of **1-CF3 isomers**.

Table 2.

Optimizing Ni^{IV}-catalyzed trifluoromethylation

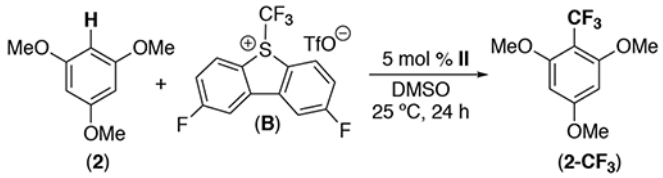

entry	modification	yield (%)[a]
1	dark	37
2	no **II**	0
3	ambient light	35
4	**I** as catalyst	25
5	**A** used as oxidant	25
6	2 equiv substrate	62
7	5 equiv substrate	93

[a]Yields determined by ^{19}F NMR spectroscopy using trifluorotoluene as an internal standard and are based on **B** as the limiting reagent. Standard conditions: 1.0 equiv **2**, 1.0 equiv **B**, 5 mol% **II** in DMSO at room temperature for 24 h.